Clustering of Fiber-Break Related Events in Carbon Fiber Reinforced Polymer Composites Using Acoustic Emission

T. Whitlow and M. Sundaresan
North Carolina A&T State University, Mechanical Engineering Dept., Greensboro, NC 24711

Abstract

The objective of this paper is to develop a technique capable to providing timely warning of the onset of critical damage events that precede the catastrophic failure of composite specimens. The sequential failure of numerous adjacent fibers is known to trigger the final fracture of composite structural elements. In this paper, the detection of the formation of such critical clusters of fiber breaks among the millions of damage events that include matrix cracks, delamination, and individual fiber breaks, is shown to be feasible through cross-correlation of acoustic emission waveforms. Acoustic emissions released during static loading of $[0/90]_{3S}$ cross-ply and $[+45/90/-45/0]_{2S}$ quasi-isotropic specimens were examined in detail for a large number of specimens.

Keywords: Fiber composites, clustering, critical damage events, cross-correlation

Introduction

Damage initiation and progression in carbon fiber reinforced composites have been well studied and is known to occur in stages and involves several failure mechanisms (e.g., matrix cracking, fiber breakage, delamination) [1 – 6]. The presence of certain mechanisms may give an indication on where along the failure process the material currently is. Each mechanism has a unique physical process in terms of duration and energy release rate which should produce distinct AE signals. The subtle differences in AE signals have been a focus for distinguishing the failure modes. Liu et al. [7] and Mechraoui et al. [8] studied the various failure mechanisms using primarily AE amplitude with each mechanism occupying a distinct amplitude range but noted that amplitude values will depend on the material system as well as the source to sensor distance. Yu et al. [9] looked at specific frequency values to monitor failure in carbon reinforced composite specimens. Bussiba et al. [10] showed that not only do the different failure modes generate unique frequencies but they also have noticeably different durations. Fiber breaks are very short duration events and are known to give rise to relatively high frequency content [11]. However, examining a given parameter may not provide sufficient information regarding the source [12] since the failure modes may occupy common parameter regimes.

The various failure modes have different effects on the integrity of the structure and can potentially be classified as either critical or non-critical damage. This ultimately depends on the make-up of the composite which dictates the failure process. Damage initiation and progression in fiber reinforced composites have been well studied in the past with several techniques utilizing micromechanics based models to predict the behavior of the material under certain load conditions. Ogi et al. [13] developed a probabilistic model to predict transverse matrix crack in cross-ply panel and compared it to experimental results. Wharmby et al. [14] related the transverse crack density to changes of the elastic modulus which is more drastic in the absence of 0˚plies. It was noticed that the majority of the stiffness reduction occurred within the first 10% of

the normalized life. Acoustic energy can also be a useful parameter to study damage progression. High energy events signify large crack growth which can be captured and characterized using acoustic emission techniques. Using cumulative AE energy was shown to agree well with C-scanning and microscopic analysis when monitoring damage accumulation [15]. Such methods have been shown to sufficiently capture the material behavior as long as the stress state information can be determined. However, there has not been a technique that focuses on identifying the onset of critical damage in real time. Even AE techniques, which attempt to distinguish between the different failure modes in real time, do not differentiate between non-critical and critical damage growth. For this study, critical damage is defined as that which indicates significant damage or directly precedes final failure.

Filtering out inconsequential signals not only allows for greater emphasis to be placed on important events but also addresses the data management issue associated with AE in unidirectional composite materials. Unidirectional composites are profuse emitter of acoustic emissions and can produce tens of thousands of signals during a simple coupon test. This can be counteracted by raising the trigger threshold to decrease the AE hit rate. Consequently, lower amplitude signals will be missed as a result. Under the assumption that critical damage signals start with low energy, ignoring lower amplitude signals may limit the ability to detect the early onset of critical damage growth. Without a filter, all relevant signals across the entire amplitude spectrum can be analyzed and also stored for later processing if necessary. The volume of AE data generated during testing may restrict the acquisition parameters used or the test duration. Ultimately, this process is a balance between determining the minimum amplitude/energy of relevant signals and staying below the maximum number of signals capable of being analyzed by post-processing software.

This work utilizes a cross-correlation technique as a filter to discriminate between non-critical and critical damage in carbon fiber-reinforced polymer (CFRP) panels while accounting for relevant low energy signals. Cross-ply and quasi-isotropic specimens were cut from laminates developed at NASA Armstrong Flight Research Center. The layups of the laminates were designed to resemble those of carbon fiber composites used in current aerospace structures. Damage evolution as it transitions from insignificant crack growth to meaningful damage was investigated using AE techniques.

Experimental

Each panel was made by stacking unidirectional tape to achieve a desired layup. Two layups were manufactured: quasi-isotropic $[45/0/-45/90]_{2S}$ and cross-ply $[0/90]_{3S}$. After each lamina were positioned and vacuumed bagged, they were heated 1.1˚C/min to 121˚C, held at that temperature for one hour then cooled at room temperature. ASTM tension test standard D3039 was used to determine the dimensions of each rectangular specimen which was 25 mm x 275 mm x 3 mm. The sensor to sensor length was approximately 108 mm and piezo-electric wafer sensors (10 mm wide, 20 mm long, 0.5 mm thick) were bonded adhesively on both ends of the gage section while damped ultrasonic transducers of 6 mm diameter were attached outside the gage to function as guard sensors (12 mm from PZT sensors). The frequency range for the PZT sensors and ultrasonic transducers was 100 to 700 kHz and 100 to 400 kHz, respectively, and no appreciable resonances were seen. Also, even though the guard sensors were more sensitive to the out-of-plane mode, their overall sensitivity was good enough to eliminate signals outside the gage. This was confirmed using lead breaks. The polarization direction for the wafer sensors was

along the width direction, which increased sensitivity to signals propagation axially in the specimen. Wideband PAC 2/4/6 preamplifiers were used and the 40 dB setting was typically used for both static and fatigue tests. All AE data was recorded on a 4-channel PCI-2 AE system and a 35 dB_{AE} threshold was used. A sampling rate of 5 MHz was used to measure waveforms of 2048 data points with a pre-trigger of 256 µs. Hit definition and hit lockout time were 100 µs and 400 µs, respectively. Five specimen from each layup were tested.

The specimens were loaded in tension using a hydraulic testing machine. Quasi-static tension tests were done at a rate of 14 MPa/min to ensure a sufficient number of AE events would be captured to characterize the separate failure regions. With the tensile strengths for the cross-ply and quasi-isotropic specimens were 965 MPa and 717 MPa respectively, each tensile test was roughly one hour. Initially, lead breaks were done to ensure each sensor had similar frequency responses and sensitivity. Also, the time of flight of signal from one sensor to the next can be measured and used to calculate the speed of sound (velocity) of the signal, which is useful in determining source location. A schematic of an instrumented specimen is shown below in Fig. 1.

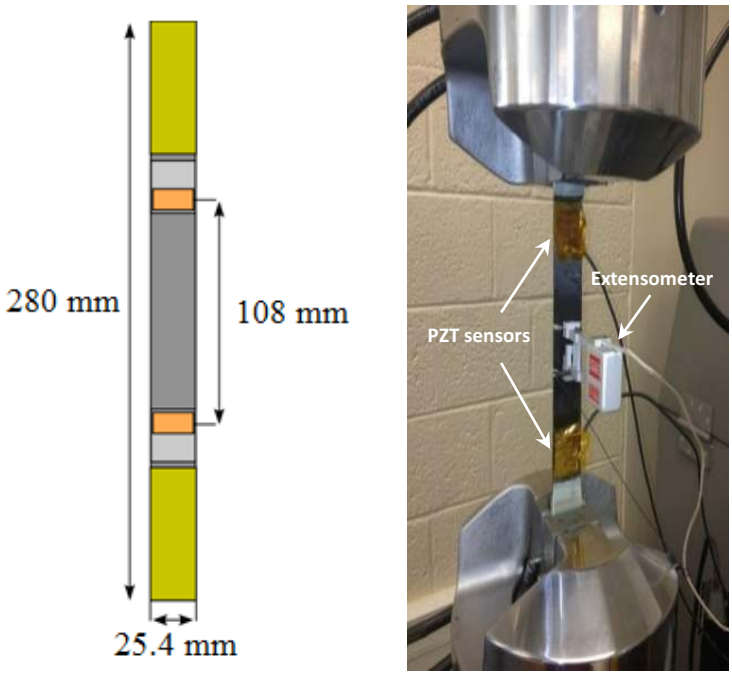

Fig. 1. Tensile specimen dimensions (left) showing dimensions of the length and sensor to sensor distance, specimen during testing.

Methodology

Each static test is capable of generating tens of thousands of signals depending on parameters such as threshold value, sensor sensitivity, and failure process of the material. This study utilized a cross-correlation technique to extract important signals based on the density of signals generated in a particular area over a set period of time. This approach relates an area where a high density of similar AE signals is being generated to critical localized damage growth. Localized damage growth is considered to be where a given source mechanism continuously grows or happens within a relatively small area or volume. In such case, that mechanism should produce repetitive signals as long as there has not been a drastic change in the medium. A focus

is placed on critical localized damage, such as fiber breaks, that significantly reduces the strength of the component. It is known that a fiber breakage causes stress redistribution into neighboring fibers which may fail if their ultimate strength is exceeded [16]. These neighboring fibers simultaneously fail in groups, or i-plets, at high load [1, 3, 6]. This behavior has been captured in great detail using computed tomography [4]. Capturing the failure of these i-plets in terms of AE clusters can provide great insight on the damage state of the material in real-time. Also, given that composites may initially exhibit random cracking, such a technique may be able to distinguish between separate localized damage areas.

The correlation process relies on raw waveform data captured by the individual sensors to determine location and various AE parameters (duration, frequency, energy, etc.). Typical AE software calculates such information but analyzing waveform data using MATLAB was found to be more effective. The cross-correlation technique *xcorr* in MATLAB used to compare separate data sets is shown below in Eqs. (1–3), (MATLAB R2013a, MathWorks Inc., Natick, MA, 2013).

$$R_{xy}(m) = E\{x_{n+m}{y_n}^*\} = E\{x_n{y_{n-m}}^*\} \tag{1}$$

$$\hat{R}_{xy}(m) = \begin{cases} \sum_{n=0}^{N-m-1} x_{n+m}{y_n}^* & m \geq 0 \\ \hat{R}^*{}_{xy}(-m) & m < 0 \end{cases} \tag{2}$$

$$c(m)=\hat{R}_{xy}(m-N) \qquad m = 1,2,\ldots 2N-1 \tag{3}$$

If there are two continuous functions representing waveform data, x and y, there will be an expected value, E, resulting from comparing the two functions. The variable m is the lag or shift, the output is the correlation array, c, and N is the number of data point in the waveform. Each correlation value corresponds to a lag value and the degree of how similar two waveforms are can be found by finding the maximum value of c. A visual representation of how this technique works is shown in Fig. 2. The first signal detected by each sensor serves as the initial reference signal and the following signals that fall within a specified window, 50 for the data presented later, are correlated to the reference. For the test data shown here, a window size of 50 yielded consistently good results. However, the necessary size will vary depending on the rate of the load applied and sensor sensitivity. This standard window length was used which cut out most of the regions of inactivity. Some events were clearly shorter or longer than this window but nearly all useful data was capture in either case. Utilizing lead breaks, a 90% correlation factor was seen to be sufficient in discriminating surface signals 2 mm apart. In the figure on the left, using waveform 1 as the reference, two red signals that follow in the window indicate they correlate at a high percentage with 1 and form a cluster of 3, including the reference. Next, signal 1 and it's two matching waveforms are removed and process repeats using waveform 2 as the reference, which forms a cluster of 4 of the following waveforms. When clustered signals are removed from the data set, the remaining signals are shifted to fill the empty spaces and the next iteration of the process begins. Each cluster is independent of one another and is sensitive to localized damage. This "on-the-fly" technique uses real time data to monitor critical damage growth and has potential to be used *in-situ*.

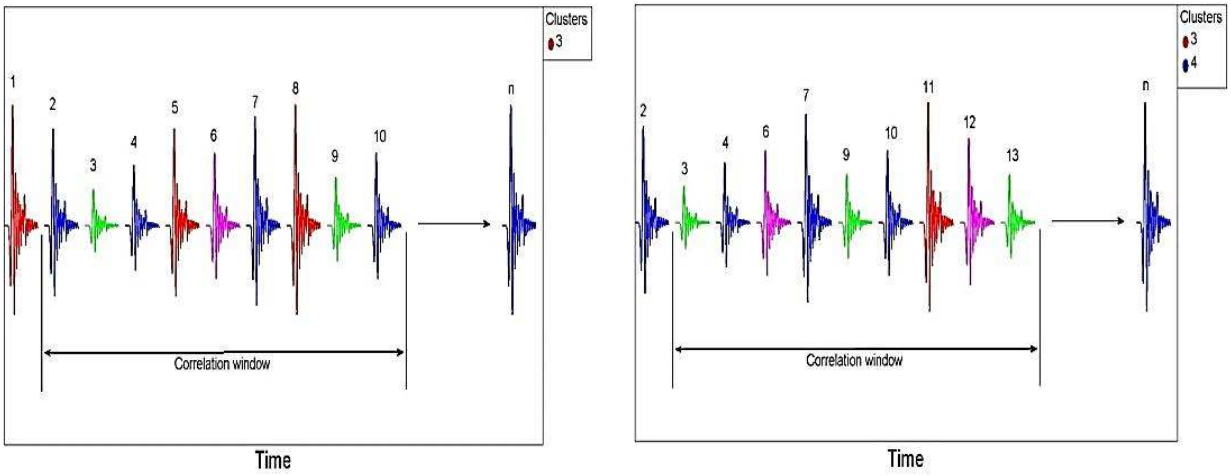

Fig. 2. Schematic of clustering process with like signals colored the same. Numbers correspond to the order that the signals were detected.

When attempting to distinguish between the various source mechanisms, there are expected parameter regimes each mechanism should occupy. However, these parameter values vary with propagation distance. Using correlation, the effects of the attenuation, dispersion, and other aspects of wave propagation on the measured waveform can be taken into account. Such as, signals of the same source type and from the same location should be nearly equally affected by the aforementioned processes. During the early onset of damage, signals that are captured within a relatively short time that correlate at a high percentage may indicate localized damage growth and as the damage becomes more pronounced, individual signals travel approximately the same path within the medium. For a finite time, the medium is assumed to not change due to damage and the signals that occur within this window that correlate at or above a predetermined percentage are, therefore, grouped into a clusters. Whereas most models require intrinsic knowledge about the state of the material to predict failure, here, the rate of cluster formation as well as cluster size was seen to be an indicator of critical damage for quasi-static tests.

Results

AE Parameters Analysis

The AE data generated during static loading for both the cross-ply and quasi-isotropic material can be seen below. Cumulative AE events vs stress plots can be seen in Fig. 3 and highlight the separate regions where matrix cracking, delamination, and fiber breaks occur at a high rate. Initially, a sudden increase in the number of events at low stress is seen due to failure of the matrix which generates a high rate of acoustic emissions. This behavior typically happens around 20-40% of the ultimate stress and saturate shortly after. Matrix cracks saturation is followed by an intermediate period characterized by minimal AE signal generation. At this point, the fibers are completely responsible for carrying load and the drastic increase of AE activity seen before failure is primarily associated with fiber breakage and delamination.

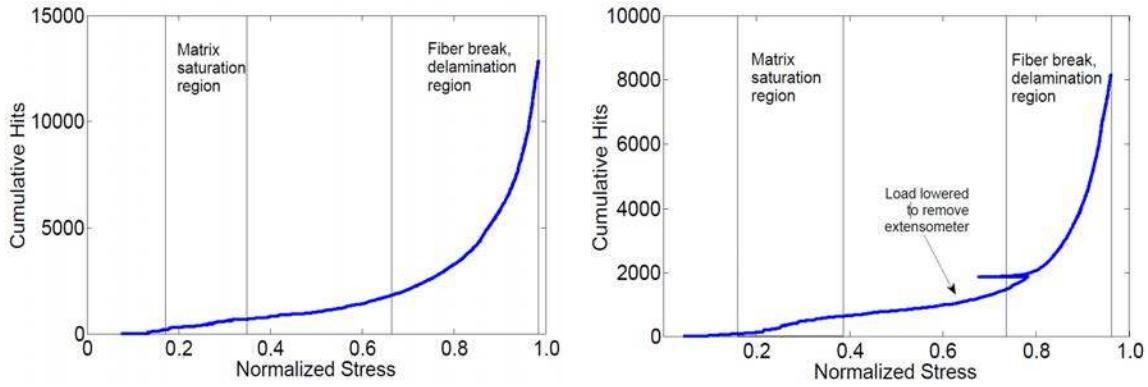

Fig. 3. Cumulative AE hits vs stress for cross-ply (left) and quasi-isotropic (right).

The above cumulative AE plots follow the expected multi-stage failure process [17] but do not show much difference between the two materials. Since the first and last regions contain extensive matrix cracking and fiber breaks, respectively, examining the AE parameters may provide information on the individual failure mechanisms. Splitting of the matrix occurs over a certain area and happens over a particular period of time whereas carbon fibers have a relatively smaller cross-sectional area and break almost instantaneously. Ideally, this difference in source duration and energy release of the failure modes should generate unique signals in terms of the traditional AE parameters.

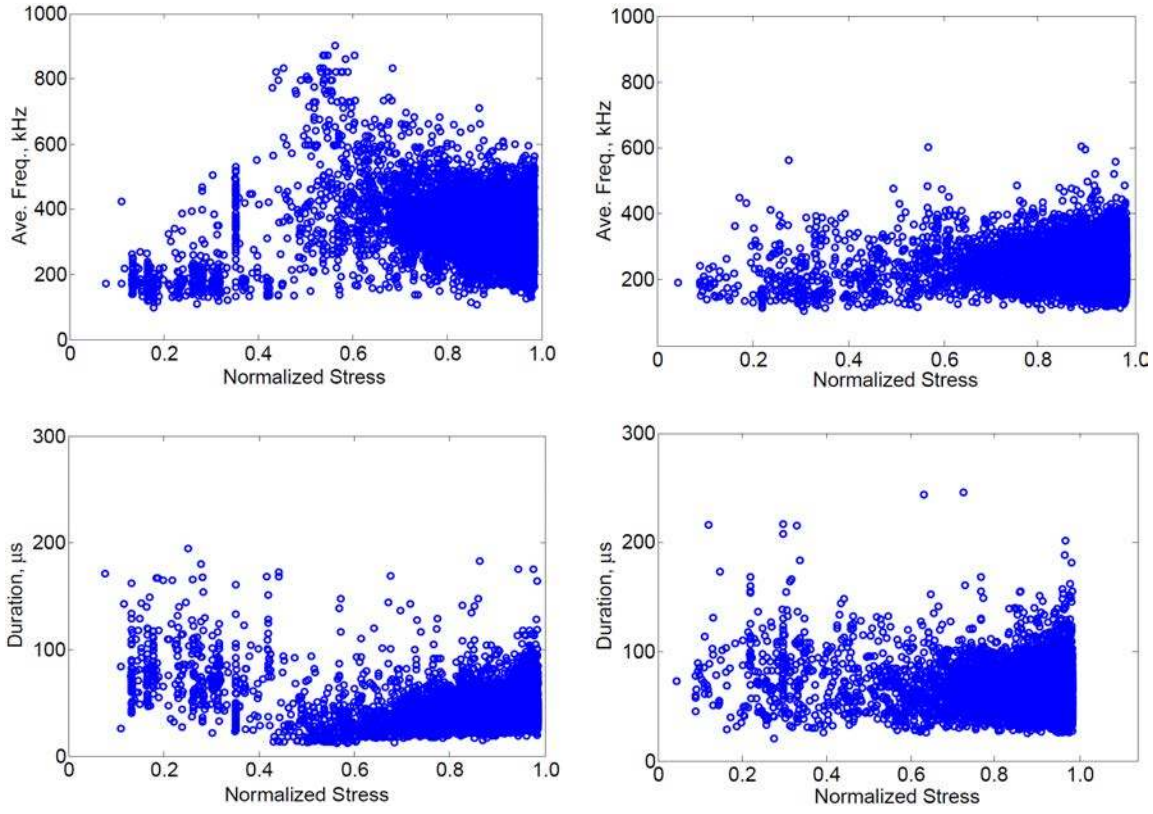

Fig. 4. Typical average frequency and duration plots seen for the two different lay-ups: cross-ply (left), quasi-isotropic (right).

Below, the average frequency and duration plots of the individual AE events, shown as blue dots in Fig. 4. The average frequency was calculated by estimating the number of cycles within a waveform in a given time window. Ideally, matrix cracking and fiber breaks should generate very distinct signals but there is only a minimal difference in the frequency characteristics seen for the two regions. This is seen in both cross-ply and quasi-isotropic material. However, the later region for the cross-ply seems to have a slightly higher average frequency than the quasi-isotropic material. Duration plots for both material as well as any other parameter plots provided very limited information on the damage development due to signals being affected by attenuation, dispersion, and scattering. The effects of attenuation and dispersion as a function of material properties and geometry have been well documented. However, the effects of attenuation and dispersion as a function of damage is not well understood because they depend on the amount of damage a signal encounters on its path to a sensor rather than the amount of overall damage.

Correlation of AE signals

Clustering of AE signals usually involves extracting parameters and forming groups or classes based on waveform characteristics. Some methods utilize un-supervised approaches that make use of amplitude or weighted metrics as classification metrics [18-21]. The accuracy of such techniques depends on accurate measurement of distinguishing features while accounting for effects of wave propagation, which is heavily dependent on distance.

The proposed correlation technique took the same data that generated limited insight from a traditional AE parameter standpoint and extracted meaningful information in terms of critical damage growth. To account for the change in the propagating medium due to damage, a window was used to only analyze successive signals to find clusters. This window, 50 successive events, assumes that the material microstructure of a given signal path stays constant or exhibits insignificant change for a finite period of time or stress. The clusters plots using a 90% correlation value are shown in Fig. 5 and detail how various cluster sizes grow as a function of stress. Each line represents an individual cluster size.

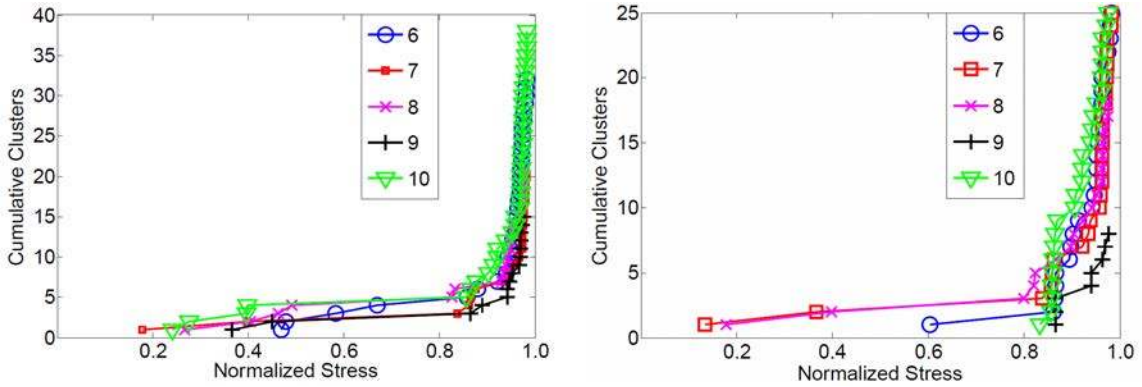

Fig. 5. Cumulative cluster growth for cross-ply specimen: sensors 1 (left) and 2 (right). Cluster sizes of 6 to 10 were plotted. This behavior was seen for quasi-specimens as well (not shown).

The most accurate and non-trivial way to accurately capture the fiber break phenomenon is to physically count the breaks using high resolution microscopy. Reifsnider and Jamison [1] manually observed fiber breakage in each ply of a cross-ply and unidirectional specimens using scanning electron microscopy (SEM). A specimen was loaded to a certain percentage of the

ultimate stress, then unloaded and dissected, and the number of fiber breaks for given area (mm^2) was determined. This was done at multiple ultimate stress percentages. Figure 6 shows a comparison between these findings and the results of this work. The AE data is a cumulative plot of AE clusters that have a size of 10 or greater. After sifting through the data, it was determined that 10 was a consistent metric for a minimal cluster size.

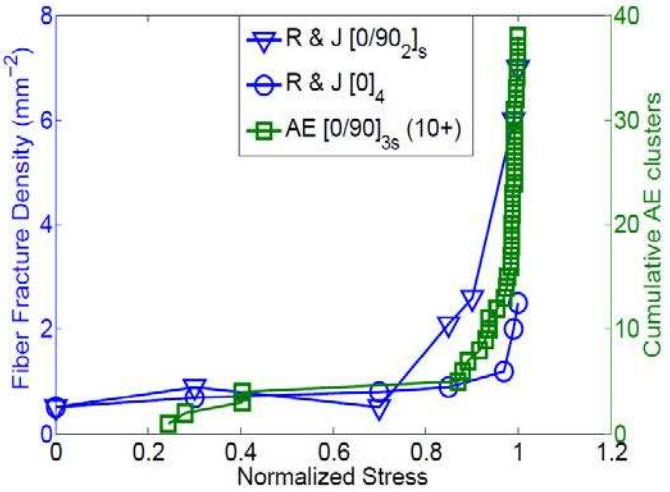

Fig. 6. Comparison of AE clusters seen in cross-ply to fiber break measurements using SEM [1].

From the above plot, the trend of the AE data falls between the SEM data as expected since the lay-up of the AE specimen falls between the layup of the other two. Having such physical evidence can provide calibration and fine tuning of the AE data analysis, which will allow this behavior to be characterized without any labor intensive or computationally heavy processes. With that being said, the ultimate comparison would involve the same specimen for AE measurement and SEM imaging.

The waveforms that make up the clusters were also examined and the AE features were studied. AE parameter analysis of clustered waveforms may provide information not noticeable when all AE data is analyzed. The frequency content of the reference waveform of each cluster was plotted with respect to stress, Fig. 7.

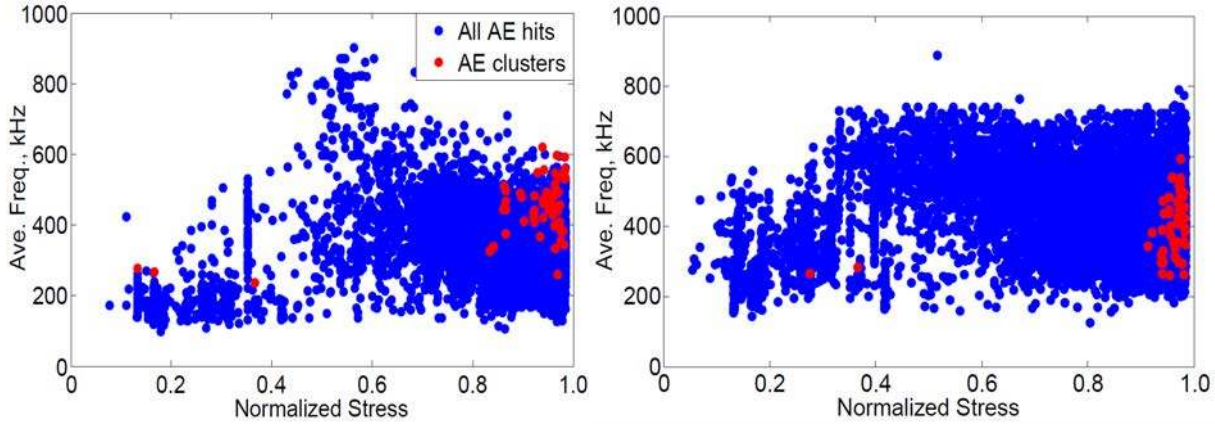

Fig 7. Average frequency of cluster signals (red) and all AE data measured in cross-ply specimen: data from sensor near failure (left), away from failure (right).

In the above average frequency plots, the reference signals (red) are superimposed over all the AE data. Since the clusters are associated with localized damage growth resulting from fiber breakage, it is expected that the signals contain relatively higher frequency content. Theoretically, fiber breaks should generate much higher frequencies than what is shown in Fig. 7 but the PZT wafer sensors had an upper frequency limit around 700 kHz. Sensors having a broader frequency response can be used but the influence of attenuation on the signals seems to play a more significant role in the measurement of higher frequencies. Hence, the reference signals from a given sensor tend to occupy the upper frequency domain when failure occurs near or at that sensor.

Location of clusters

The process of identifying clusters started with understanding localized damage growth. In this section, the origin of AE signals is studied and determined. Location of AE events itself is a well-understood process and has been studied extensively. In the case of transient waves, individual sensors may be triggered by different parts of the same waveform. A detailed waveform analysis was done to mitigate this problem and help enhance source location of AE clusters. Such as, when an event is captured by the two sensors, both waveforms are analyzed to insure that each sensor was triggered by the leading peaks. This provided a safeguard against measuring incorrect time of arrival which affects the ability to accurately locate the events.

Since clusters are composed of multiple signals, source location only applies to the reference waveform and the subsequent signals are assumed to have originated from the same location. To verify that the clusters originated from the same location, random waveforms from various clusters were chosen and located. The transient nature of the signals makes it difficult to get precise time of arrival measurements. The extensional mode, given its faster velocity and non-dispersive nature over the frequency*thickness range of interest, was used to determine the velocity of the wave, which was found to be approximately 5000 m/s. However, as in the case of an aluminum plate, the in-plane surface displacement of the extensional mode is usually inversely proportional to its frequency, with most of the energy of the in-plane component being contained near the mid-plane of the material; the opposite effect is seen for the out-of-plane component of the extensional mode [22]. The PZT wafer sensors used are designed to be much more sensitive to the in-plane component but there is only a small percentage of in-plane energy available for measurement. The internal structure of composite materials is quite different from isotropic media but this phenomenon may have also influenced AE measurements in this study.

Figure 8 shows the location of raw AE data and the corresponding signal density plots relative to sensor placement. While it is possible to notice some areas of higher AE activity, the copious nature of polymer matrix composites can mask useful information due to the sheer number of events. The density plot highlights regions of high localized activity that is not clearly visible in the raw data. The density scale is based on the number of AE clusters per square mm, with dark areas corresponding to regions of high AE activity. These clustered signals are the targets of the correlation technique and can be indicators of critical damage growth. In addition, having location information gives the ability to see where the specimen will fail in real time.

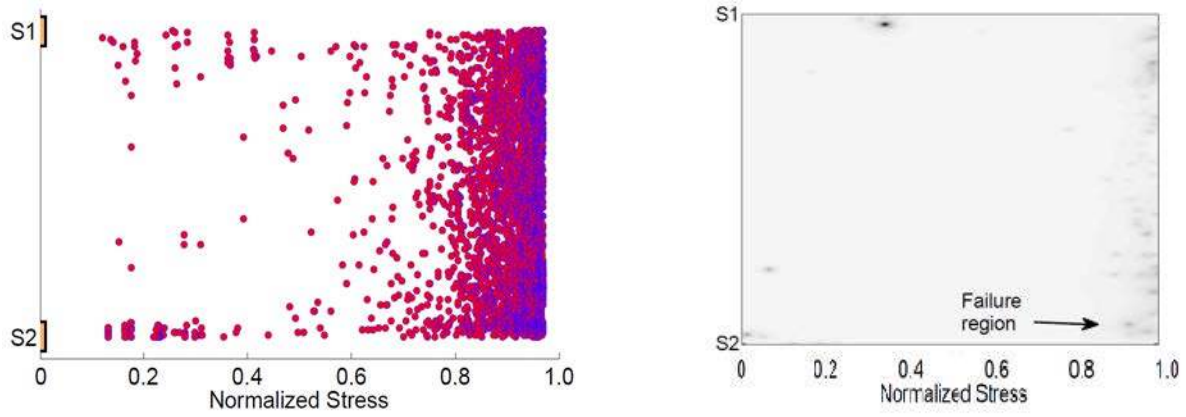

Fig. 8. Raw AE location data for unclustered data (left) and signal density of the unclustered data (right) plots for cross-ply specimen. S1 and S2 refer to sensors 1 & 2, which were 75 mm apart. Events are the individual dots. The black area in right plot is due to dense AE activity.

The above plot shows the raw location of AE events as the specimen was loaded to failure. Tens of thousands of signals were measured but the events were seemingly distributed randomly along the gage section. Using only location, there was not a relative clustering of signals near the failure region which would be noticeable in the density plot on the right. However, there was useful information extracted from the above data using correlation and it was plotted in the form of clusters, seen below.

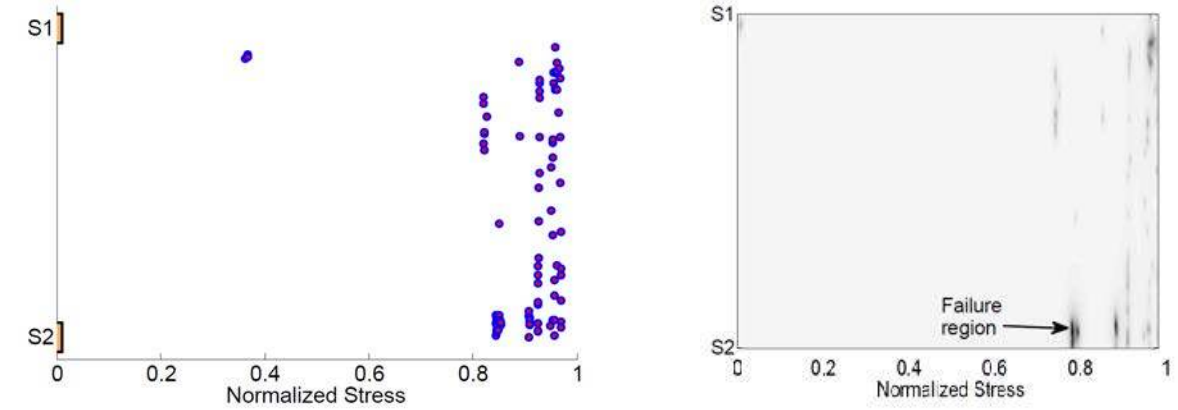

Fig. 9. Raw AE cluster location for clusters of 10 (left) seen in cross-ply specimen. Right figure shows the cluster location data transformed into a cluster density plot to highlight the location of clusters.

Figure 9 shows the results of applying the correlation technique to raw AE data. Whereas the raw data and the AE parameter data gave very limited insight, the cluster based approached provided indication of critical damage growth as well as location information. Failure of the specimen occurred slightly above sensor 2 which corresponds well with the dense region of AE clusters. On the color spectrum, black indicates an area of high cluster density. The two dense clusters align well with the failure area but slightly less dense clusters appear near sensor 1 right before failure. Ideally, the location of the clusters should indicate where the material will fail. However, the uncertainty associated with the material in terms of its internal structure, Lamb

wave behavior, and even the speed of sound right before sudden failure is not well understood and requires more investigation.

Conclusions

Quasi-static tension tests were performed on cross-ply and quasi-isotropic CFRP specimens. The traditional acoustic emission parameters, such as frequency and duration, were examined for information pertaining to the different types of damage growth during testing. While slight differences were noticed in the average frequency and duration plots of the matrix crack saturation region and the fiber break region for the cross-ply material, there was too much scatter in the data to quantify anything useful. The AE parameter analysis for the quasi-isotropic data was unable to highlight the different failure regions as well.

A correlation technique was developed to extract localized damage growth information associated with critical damage growth. Using the same AE data that yielded minimal information from traditional parameter analyses, the correlation process was able to extract localized clusters which are assumed to be related to fiber failure. The results were consistent and repeatable for both layups and verified on multiple specimens. This technique was able to monitor the development and growth of various clusters sizes and found that the occurrence of large clusters directly precedes sudden failure.

Acknowledgements

The authors acknowledge NASA Armstrong Flight Research Center for supporting this work.

References

1. Reifsnider, K.L., & Jamison, R., *Fracture of Fatigue-Loaded Composite Laminates.* International Journal of Fatigue, 1982. **4**(4): 187-197.
2. De Rosa, I., C. Santulli, and F. Sarasini, *Acoustic emission for monitoring the mechanical behaviour of natural fibre composites: A literature review.* Composite: Part A, 2009. **40**: 1456-1469.
3. Thionnet, A., H.Y. Chou, and A. Bunsell, *Fibre break processes in unidirectional composites.* Composites: Part A, 2014. **65**: 148-160.
4. Scott, A., I. Sinclair, M. Spearing, A. Thionnet, and A. Bunsell, *Damage accumulation in a carbon/epoxy composite: Comparison between a multiscale model and computed tomography experimental results.* Composite: Part A, 2012. **43**: 1514-1522.
5. Morton, H., P. Reed, A. Scott, I. Sinclair, and M. Spearing, *Quantification of carbon fibre/epoxy resin composite failure processes using synchrotron radiation computed tomography.* ECCM15-15th European conference on composite materials, 2012.
6. Foster, G., *Tensile and Flexure Strength of Unidirectional Fiber-Reinforced Composites: Direct Numerical Simulations and Analytic Models* (Master's Thesis), in *Department of Engineering Science and Mechanics*. 1998, Virginia Polytechnic Institute and State University.
7. Liu, P.F., J.K. Chu, Y.L. Liu, and J.Y. Zheng, *A study on the failure mechanisms of carbon fiber/epoxy composite laminates using acoustic emission.* Materials & Design, 2012. **37**: 228-235.
8. Mechraoui, S.-E., A. Laksimi, and S. Benmedakhene, *Reliability of damage mechanism localisation by acoustic emission on glass/epoxy composite material plate.* Composite Structures, 2012. **94**(5): 1483-1494.
9. Yu, Y.-H., J.-H. Choi, J.-H. Kweon, and D.-H. Kim, *A study on the failure detection of composite materials using an acoustic emission.* Composite Structures, 2006. **75**(1-4): 163-169.

10. Bussiba, A., M. Kupiec, S. Ifergane, R. Piat, and T. Bohlke, *Damage evolution and fracture events sequence in various composites by acoustic emission technique.* Composites Science and Technology, 2007. **67**: 1144-1155.
11. Jong, H.J., *Transverse Cracking in a Cross-ply Composite Laminate - Detection in Acoustic Emission and Source Characterization.* Journal of Composite Materials, 2005. **40**(1): 37-69.
12. Gorman, M., *Modal AE analysis of fracture and failure in composite materials, and the quality and life of high pressure composite pressure vessels.* Journal of Acoustic Emission, 2011. **29**: 1-28.
13. Ogi, K., S. Yashiro, and K. Niimi, *A probabilistic approach for transverse crack evolution in a composite laminate under variable amplitude cyclic loading.* Composites Part A: Applied Science and Manufacturing, 2010. **41**(3): 383-390.
14. Wharmby, A., *Observations on damage development in fibre reinforced polymer laminates under cyclic loading.* International Journal of Fatigue, 2003. **25**(5): 437-446.
15. Bourchak, M., I. Farrow, I. Bond, C. Rowland, and F. Menan, *Acoustic emission energy as a fatigue damage parameter for CFRP composites.* International Journal of Fatigue, 2007. **29**(3): 457-470.
16. Blassiau, S., A. Thionnet, and A. Bunsell, *Micromechanisms of load transfer in a unidirectional carbon fibre-reinforced epoxy composite due to fibre failures. Part 2: Influence of viscoelastic and plastic matrices on the mechanisms of load transfer.* Composite Structures, 2006. **74**: 319-331.
17. Reifsnider, K.L. and S.W. Case, *Damage tolerance and durability of material systems*. 2002: Wiley Interscience.
18. Marec, A., J.H. Thomas, and R. El Guerjouma, *Damage characterization of polymer-based composite materials: Multivariable analysis and wavelet transform for clustering acoustic emission data.* Mechanical Systems and Signal Processing, 2008. **22**(6): 1441-1464.
19. Godin, N., S. Huguet, R. Gaertner, and L. Salmon, *Clustering of acoustic emission signals collected during tensile tests on unidirectional glass/polyester composite using supervised and unsupervised classifiers.* NDT & E International, 2004. **37**(4): 253-264.
20. Loutas, T. and V. Kostopoulos, *Health monitoring of carbon/carbon, woven reinforced composites. Damage assessment by using advanced signal processing techniques. Part I: Acoustic emission monitoring and damage mechanisms evolution.* Composites Science and Technology, 2009. **69**(2): 265-272.
21. Sause, M.G.R., A. Gribov, A.R. Unwin, and S. Horn, *Pattern recognition approach to identify natural clusters of acoustic emission signals.* Pattern Recognition Letters, 2012. **33**(1): 17-23.
22. Rose, J., *Ultrasonic Waves in Solid Media*. 1999. Cambridge University Press.